Effect of organic coatings on optical properties of black carbon aerosol: Insights from Mie theory based model simulations

Tejas Rathod[1] and Sanjay Sahu[1, 2*]

[1]Environmental Monitoring and Assessment Division, Bhabha Atomic Research Centre, Mumbai- 400085, India

[2]Homi Bhabha National Institute, Mumbai- 400094, India.

*Corresponding author: Tel: +912225592375

E-mail address: sksahu@barc.gov.in

Abstract

Black carbon (BC), play a crucial role in climate change due to their significant impact on radiative forcing. This study investigates the influence of organic carbon (OC) coatings on the optical properties of BC aerosols using Mie theory-based calculations. We have examined a range of core diameters and coating thicknesses to assess changes in both absorption and scattering cross-sections. The results reveal that coatings consistently enhance both absorption and scattering properties, with the enhancement in scattering being higher in magnitude than enhancement in absorption. The study compares the optical properties of coated BC with that of OC particle having same dimensions, showing that as the coating thickness increases, the optical behavior of the coated BC particle converges towards that of OC. The calculations for radiative forcing efficiency showed that as the coating on BC was increased, its forcing efficiency decreased, implying that organic coated BC may have a reduced radiative impact in the atmosphere.

Keywords: black carbon, organic carbon, enhancement ratio, radiative forcing, mie theory

1. Introduction

Aerosols play a crucial role in atmospheric radiative forcing by interacting with incoming solar and outgoing terrestrial radiation. Their overall effect on Earth's energy balance depends on whether they scatter or absorb radiation. Scattering aerosols increase the planetary albedo and lead to negative radiative forcing (cooling effect), whereas absorbing aerosols decrease albedo and result in positive radiative forcing (warming effect). Globally, aerosol forcing remains one of the largest uncertainties in estimating total anthropogenic radiative forcing and future climate projections [1]. Among various aerosol types, BC is a strong absorber of solar radiation and contributes positively to radiative forcing. It is among the top anthropogenic contributor, along with CO_2 and methane, with an estimated effective radiative forcing (ERF) of 0.11 W m^{-2}, and a likely range of –0.20 to +0.42 W m^{-2}, reflecting both positive and negative values after accounting for cloud, lapse-rate, and atmospheric water-vapor adjustments [1, 2]. In contrast, OC aerosols, the other major type of carbonaceous aerosol, are primarily scattering in nature and generally exert a negative radiative forcing, with an emissions-based ERF of –0.21 W m^{-2} and a range of –0.44 to +0.02 W m^{-2}, where the small positive contribution arises from

light-absorbing organic compounds, often referred to as brown carbon (BrC) [1]. These ranges highlight the substantial uncertainties in aerosol forcing estimates, which arise from variations in optical properties, morphology, mixing state, and atmospheric aging, as well as from interactions with clouds and the cryosphere [1-6]. The evolving nature of these aerosol characteristics during transport makes the degree of absorption and scattering highly variable. Such uncertainties directly impact climate model predictions of temperature responses, radiative fluxes, and the assessment of mitigation strategies for anthropogenic aerosols.

In the atmosphere, BC is typically co-emitted with OC during combustion, which leads to external and internal mixing states. In internal mixing, the OC vapors can get condensed on the BC substrate, leading to the complete or partial encapsulation of BC. In external mixing, BC and OC remain separated but get mixed externally. The evaluation of BC optical properties remains restricted due to the significant uncertainties associated with BC morphologies and mixing states [5, 7, 8]. The internal mixing state of BC has been extensively investigated for its light absorption properties [9, 10]. Theoretical calculations using the Mie core-shell model have shown that when BC is coated with OC, then the shell acts as a lens to increase the overall absorption properties of BC. This is termed the lensing effect [11]. Experimentally, thermal heating methods have been used to study this absorption enhancement [12]. Heating the aerosol at preset temperature leads to the removal of coatings from BC substrate. The ratio of absorption coefficients measured before and after removal of organic coatings provides the absorption enhancement ratio E_{abs}. Both laboratory experiments and field measurements show increased absorption due to coatings on BC, leading to E_{abs} greater than 1 [12, 13, 14, 15]. However, the coatings on BC, along with its absorption, are expected to alter its scattering properties as well. The changes in scattering properties due to coating are comparatively less explored. Few laboratory measurements have reported enhancement in BC's light scattering upon coating [16, 17, 18]. Similar to case of absorption enhancement, the enhancement in light scattering can be expressed in the form of scattering enhancement ratio E_{sca}. In terms of absolute magnitude, E_{sca} observed in these experimental studies was higher than E_{abs}. In order to estimate radiative forcing potential, along with absorption, scattering as well plays an equally important role. Climate models, which include enhancement in BC absorption due to its mixing state, often assume an E_{abs} value of ~1.5 - 2 for its radiative forcing estimation [10, 19]. However, the changes in the scattering properties of coated BC particles and their potential effect on radiative forcing capabilities remain contentious and unaddressed.

In this study, we have performed Mie theory calculations on the core-shell model to estimate changes in both absorption and scattering properties of coated BC spheres. The study focuses on the implications of OC coating on the overall optical properties of BC, providing insights into how these changes may affect radiative forcing potential. By examining both absorption and scattering enhancements, could help in improving the accuracy of radiative forcing estimates and contribute to a better understanding of BC's role in climate change impact.

2. Methods

2.1.Model configurations

The spherical core–shell model was investigated using the Mie theory–based PyMieScatt computational package [20], which provides exact solutions for the scattering and absorption of light by spherical particles. In this study, internally mixed aerosols were represented by a BC core and an OC shell. This configuration is physically plausible, as organic species can

condense on the insoluble BC core either immediately after emission or during subsequent atmospheric aging [21]. The core–shell model has been widely used in previous studies to investigate light–particle interactions and BC optical properties [9, 10, 22, 23]. While this model offers a convenient and computationally efficient framework for examining the optical behavior of internally mixed aerosols, it assumes homogeneous and concentric spherical particles. This idealization neglects real-world complexities such as non-spherical or aggregated BC morphologies, partial coatings, and variable refractive index distributions within particles. These deviations can lead to discrepancies between modeled and observed optical properties, particularly for quantities such as the absorption enhancement factor (Eabs) and single scattering albedo.

Nevertheless, Mie theory–based core–shell simulations remain valuable for quantifying first-order effects of coating and particle size on light absorption and scattering, and they continue to serve as the foundation for many regional and global climate models. However, it is important to recognize that the idealized nature of the core–shell morphology can lead to an overestimation of absorption enhancement and radiative forcing [15, 16, 24, 25]. Observational and microscopic analyses indicate that actual BC-containing aerosols often deviate significantly from this geometry. Consequently, the enhancement ratios and radiative forcing estimates derived in this study should be interpreted as upper-limit scenarios for coated BC particles. Despite these limitations, the Mie-based approach continues to provide essential insights into the sensitivity of aerosol optical properties to coating effects and serves as a benchmark for more complex modeling techniques such as the discrete dipole approximation and T-matrix methods [26].

The core diameter was varied from 10 nm to 500 nm, and the shell thickness was varied from 10 nm to 1000 nm. The wide range of core and shell thicknesses considered here is expected to include most of the observable size range of BC in the atmospheric aerosol [10]. The parameters considered for the simulation are compiled in Table 1. The study primarily discusses the optical properties of the coated BC at 550 nm, which is near the center of the visible light solar spectrum. Most of the optical measurements of aerosols are reported at 550 nm, so it makes simulation findings relevant and easily comparable with a large body of existing literature. However, the calculations were also performed for other wavelengths at 350 nm, 450 nm, and 650 nm, and compiled as supplementary information. The refractive indices at 550 nm for BC and OC were taken as 1.95 + 0.79i [30] and 1.60 + 0.0083i, respectively. The choice of the imaginary part of the refractive index (κ) for OC was based on values reported in literature (Table S1). The real part (n = 1.60) was selected consistent with previous studies [27, 28, 29]. To account for variability in OC absorption, we performed a sensitivity analysis using a range of imaginary refractive index values (κ_{OC} = 0.00001–0.03) at 550 nm, representative of purely scattering to strongly absorbing brown carbon (BrC) [31]. The real part of the refractive index was fixed at n = 1.60, consistent with literature-reported values for OC. In this sensitivity analysis, we systematically examined the effect of varying κ on the absorption and scattering enhancements of BC particles coated with OC.

2.2.Enhancement calculations

Based on the calculated absorption cross-section, the E_{abs} for a given BC core was estimated using following equation:

$$E_{abs} = \frac{C_{abs\_coated}}{C_{abs\_uncoated}}, \quad (1)$$

where C_{abs_coated} is the absorption cross-section of coated BC sphere and $C_{abs\_uncoated}$ is the absorption cross-section of uncoated BC sphere with core diameter remaining unchanged.

On similar lines the enhancement in scattering due to organic coatings was estimated in terms of E_{sca} using following equation:

$$E_{sca} = \frac{C_{sca\_coated}}{C_{sca\_uncoated}}, \quad (2)$$

where C_{abs_coated} is the scattering cross-section of coated BC sphere and $C_{abs\_uncoated}$ is the scattering cross-section of uncoated BC sphere with core diameter remaining unchanged.

It is important to note that we are comparing coated BC with uncoated BC for the same core size. However, to isolate the effect of coating on the standalone optical properties of BC, the contribution of the shell to absorption and scattering must ideally be removed. Some studies have attempted to estimate the shell contribution to absorption using linear algebraic methods [31, 32]. In these approaches, the absorption due to the shell is derived by subtracting the absorption cross section of a "bare" OC particle from that of a "coated" OC particle, where the morphologies correspond to those of bare and coated BC, respectively. However, since light absorption is not linearly dependent on particle size or morphology, these methods only provide an approximate estimate of the shell absorption and do not represent the true absorption capacity of the coating. Moreover, these methods are less suitable for assessing scattering properties, which are even more sensitive to particle size and morphology [33]. Therefore, to accurately assess the standalone optical properties of BC, more advanced numerical methods or direct experimental validation are required to better quantify the shell contribution. In the present study, we focus on the consolidated optical properties of coated and uncoated BC particles to understand their overall radiative behavior. Additionally, the simulations are extended to compare coated BC with standalone organic aerosol for different size configurations.

2.3 Radiative forcing implications

The effect of change in scattering potential due to coatings on BC aerosol can significantly impact its radiative forcing potential. The simple forcing efficiency (SFE) proposed by Bond and Bergstrom 2006 [34], is given as

$$SFE = -\frac{1}{4} F_T \tau^2 (1 - A_c)(2(1 - R_s)^2 \beta . MSC - 4R_s . MAC), \quad (3)$$

where F_T is the solar irradiance, τ is the atmospheric transmission, A_c is the cloud fraction, R_s is the surface albedo which will depend on the location of the aerosols, β is the backscatter fraction estimated using Mie calculation, and MSC and MAC are the mass scattering and mass absorption cross sections per gram, respectively. MSC and MAC can be estimated from the scattering and absorption cross-sections by normalizing them by their mass. The mass of coated and uncoated BC particle was estimated using the density provided in Table 1. The SFE Eq. can be framed to include wavelength dependence as stated following equation:

$$\frac{d(SFE(\lambda))}{d\lambda} = -\frac{1}{4}\frac{dF_T(\lambda)}{d\lambda} \tau^2(\lambda)(1 - A_c)(2(1 - R_s)^2 \beta(\lambda) . MSC(\lambda) - 4R_s . MAC(\lambda). \quad (4)$$

This equation is used to investigate the effects of changes in absorption and scattering properties due to coatings on BC sphere at 550 nm. Here, $\frac{dF_T\lambda}{d\lambda}$ was obtained from the ASTM G173-03 Reference Spectra. The cloud fraction A_c was taken as 0.6 and surface albedo R_s was taken as 0.19 [35]. The results of this study will provide valuable insights into the impact of BC coatings on radiative forcing potential, helping to improve climate models and predictions.

Table 1 *List of parameters used for Mie theory calculations in this study*

Parameters	Value	Reference
Core diameter range	10 nm to 500 nm	-
Shell thickness range	10 nm to 1000 nm	-
Wavelength	550 nm	-
Refractive Index 550 nm		-
BC	1.95 + 0.79 i	Bond and Bergstrom, 2006 [34]
OC	1.60 + 0.0083 i	Refer Table S1
Density		
BC	1.8 g cm^{-3}	Bond et al., 2006 [10]
OC	1.1 g cm^{-3}	Schkolnik et al., 2007 [36]

3. Results and discussion

3.1 Enhancement in absorption and scattering cross-section

The optical cross-sections calculated using Mie theory were used to estimate E_{abs} and E_{sca} values using Eq. 1 and Eq. 2, respecively. In our study, the Eabs and Esca were calculated for a wide range of core–shell configurations to systematically explore the theoretical parameter space. The E_{abs} was consistently greater than 1 for all non-zero coating thicknesses examined in this study, a result that aligns with prior experimental and theoretical studies [3, 12, 32, 37]. The variation in E_{abs} for various combinations of core and coated thickness is shown in Fig. 1. The increase in absorption cross-section for coated BC spheres is due to the lensing effect [31]. For a given core size, E_{abs} increased with the increase in coat thickness. The smallest core size and largest coating thickness configuration exhibited the highest E_{abs}. This suggests that the thickness of the coating on the BC sphere plays a significant role in enhancing absorption. Fig. 1 present results for the full theoretical parameter space, including extreme coating factors, which show very high Eabs values. Similar trends for extreme absorption enhancements at very high coating factors were also predicted by Bond et al. (2006) [10] using Mie theory for lognormal BC distributions. However, for realistic coating factors, the E_{abs} values obtained were physically plausible. For illustration purposes, we show E_{abs} for a 120 nm BC core, corresponding to the typical BC core sizes of aged biomass-burning aerosols reported in the literature [38, 39]. A coating factor range of 1–3 was considered to represent realistic atmospheric conditions [38]. It can be seen in Fig. S1 that the obtained E_{abs} values (1-3) are plausible and consistent with both theoretical expectations and experimental observations [3, 12, 32, 37]. The enhancement values obtained in this study are theoretical estimations for change in absorption cross-section due to coating for a single sphere. However, for an experimental setup in real scenarios, the values of E_{abs} represent an ensemble of coated particles with complex morphologies. For more accurate resemblance to a real-world scenario, advanced

simulation methods need to be explored, which is beyond the scope of the present investigation. However, the core shell model with Mie theory solutions is widely employed and it does provide valuable insights that can suggest accurate further studies.

Analogous to absorption cross-section, the scattering cross-section of coated BC was also found to be higher than the uncoated BC sphere. The increase in scattering cross-section is due to an increase in physical dimension caused by organic coating which is predominantly scattering in nature. The increase in scattering cross-section with coating thickness indicates that the presence of a coating can enhance the scattering of radiation by BC particles in the atmosphere. The net effect was the E_{sca} being greater than 1 for non zero coating thickness. The data presented in Fig. 2 illustrates the relationship between core and coating thickness on the E_{sca}. The variation pattern of E_{sca} with respect to core diameter and coat thickness is similar to that observed for E_{abs}. The E_{sca} typically increased with an increase in coat thickness for any given core size. The E_{sca} was equal to 1 for no coating configuration across all the core sizes as expected. Smaller core sizes combined with thicker coatings exhibited extreme Esca values, similar to the trends observed for Eabs. However, for realistic coating factors, the Esca values were physically plausible. Figure S1 also illustrates E_{sca} for a representative case of a 120 nm BC core, where Esca reaches approximately 14 at a coating factor of 2. The Rayleigh–Debye–Gans theory for coated fractal aggregates by Lefevre et al. (2019) [16] similarly predicts that Esca for soot can exceed 10 for organic coating fractions greater than 60% (corresponding to an effective coating factor of ≈ 2.2) and can surpass 50 for 100% organic coating (effective coating factor ≈ 3), depending on the wavelength.

Compared to E_{abs}, the magnitude of E_{sca} was higher. Fig. 3 illustrates how the ratio of E_{sca} to E_{abs} changes with core size and coating thickness. For most configurations of core size and coating thickness, this ratio was typically greater than 1. However, in cases of high core size combined with very low coating thickness, the enhancements in absorption and scattering were comparable and close to 1. This suggests that the organic coating on BC has a more pronounced effect on its scattering properties than on its absorption properties, a finding that is supported by previous experimental studies [16, 17, 18]. It highlights the critical role of coating thickness in modulating the scattering properties of BC aerosols.

A similar pattern of variation in absorption and scattering enhancements with different core and coating configurations was observed at the other wavelengths of 350, 450, and 650 nm, as illustrated in Fig. S2 and Fig. S3. For all core–shell combinations at these wavelengths, both E_{abs} and E_{sca} remained greater than 1 for non-zero coating thicknesses, consistent with the trends observed at 550 nm. Furthermore, as at 550 nm, E_{sca} was generally larger than Eabs for most combinations of core diameter and shell thickness, highlighting the more pronounced effect of the organic coating on scattering compared to absorption. These results indicate that the presence of an organic coating consistently enhances the optical cross-sections of BC across the studied spectral range, with the magnitude of enhancement depending on both the core size and coating thickness.

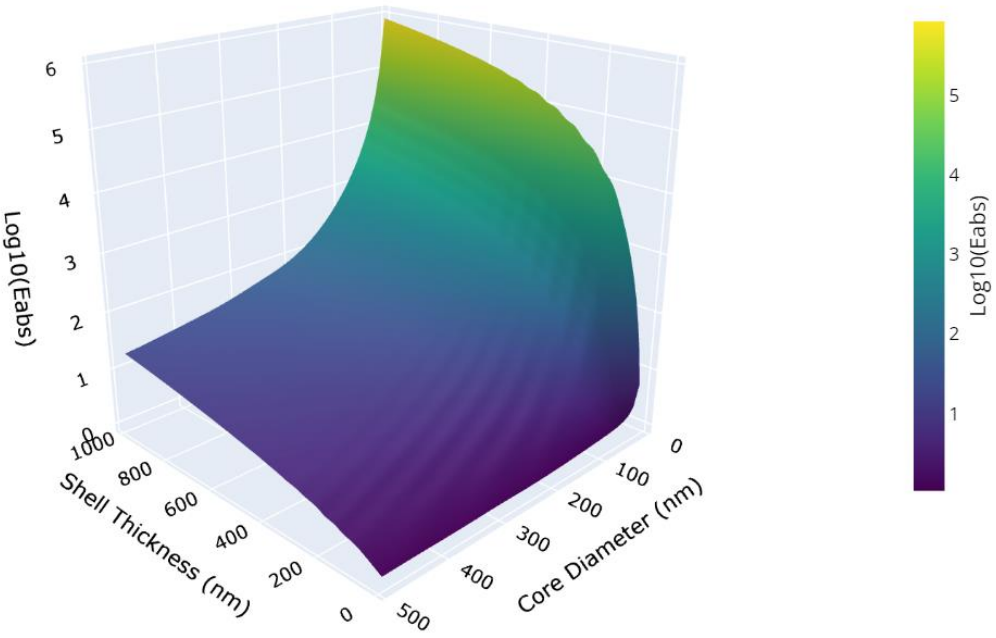

234

235 Fig. 1 Enhancement in absorption cross-section due to organic coating on black carbon core

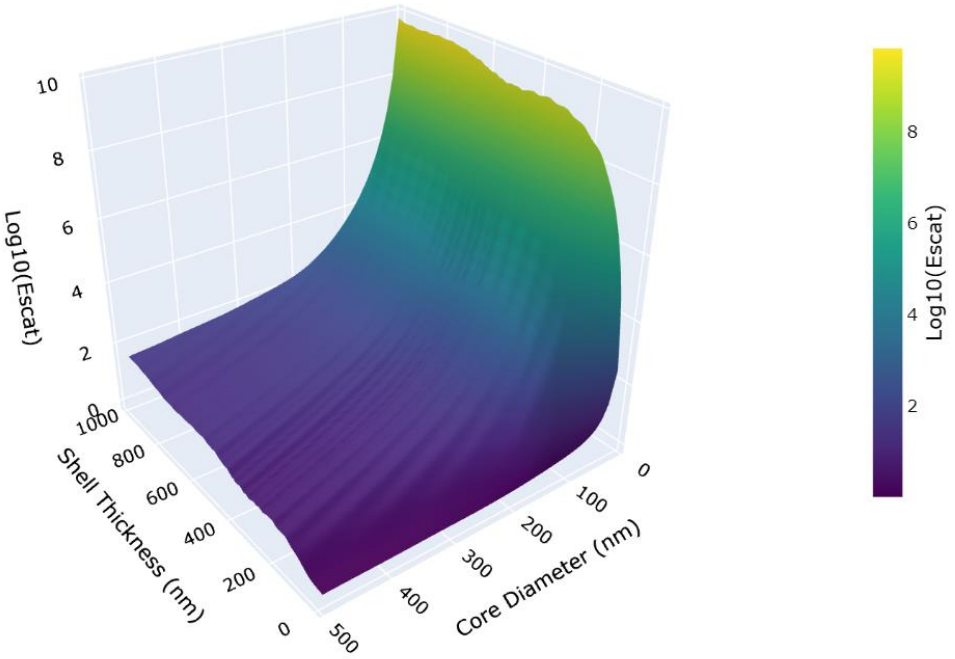

236

237 Fig. 2 Enhancement in scattering cross-section due to organic coating on black carbon core

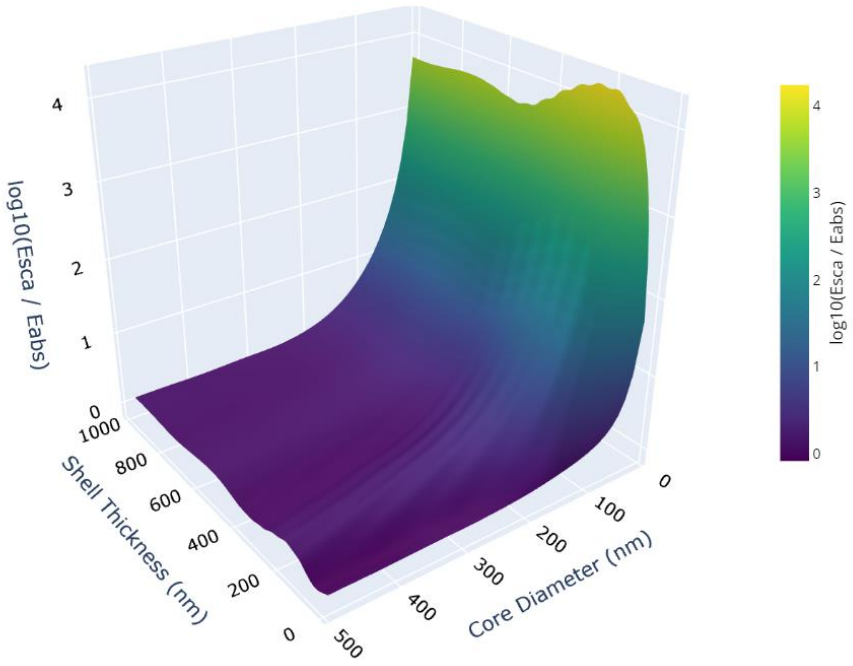

Fig. 3 Comparision of enhancement in scattering and absorption cross-section due to organic coating on black carbon core

In general, the absorption enhancement (E_{abs}) was higher at shorter wavelengths across all core and shell combinations, reflecting the stronger absorption contribution from the OC shell in the near-UV and visible range. Conversely, at longer wavelengths, the shell becomes more transparent, reducing its direct contribution to absorption. To further illustrate this wavelength-dependent behavior, a representative case of a 120 nm BC core coated with a 50 nm OC shell is shown in Fig. 4. The absorption enhancement decreases from 1.78 at 350 nm to 1.49 at 650 nm, reflecting the strong absorption of the OC shell at short wavelengths (κ_{OC}~0.0693 at 350 nm), which diminishes as the shell becomes increasingly transparent at longer wavelengths (κ_{OC}~0.0033 at 650 nm). In contrast, the scattering enhancement increases from 3.4 to 5.8 over the same wavelength range because the reduction in shell absorption allows the shell to contribute more effectively to scattering, and the coated particle's larger effective size reduces the wavelength dependence relative to the bare core. These results demonstrate the competing effects of shell absorption and size augmentation on the optical properties of coated BC aerosols and highlight the importance of wavelength in determining their radiative impact. These trends demonstrate the competing effects of shell absorption and size augmentation on the optical properties of coated BC aerosols. The overall change in absorption and scattering cross-section due to coatings provides valuable insights for understanding the optical behavior of coated BC particles in the atmosphere.

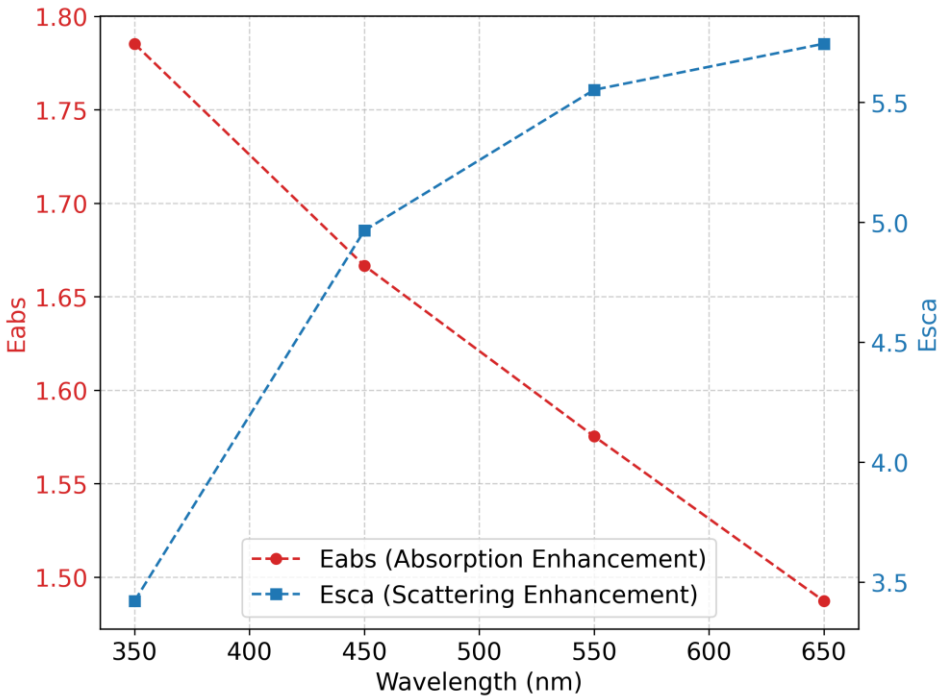

Fig. 4 Wavelength dependence of absorption and scattering enhancement for a 120 nm black carbon core with a 40 nm organic carbon shell.

To examine the sensitivity of optical enhancement due to the choice of imaginary part of the complex refractive index (κ) of an organic shell coating BC cores, we varied the imaginary part of the OC shell, while keeping the real part fixed at 1.60. The κ values ranged from 0.00001 (representing purely scattering OC) to 0.03, corresponding to strongly absorbing BrC, as categorized by Feng et al. (2013) [30]. The results shows that as κ increased, absorption enhancement rose steadily (refer Fig. S4). This trend shows that as the shell becomes more absorbing, it contributes more directly to the overall absorption of the particle system. The lensing effect wherein the coating focuses light onto the absorbing BC core remains active, and the added shell absorption compounds the enhancement. In contrast, scattering enhancement was largely insensitive to the imaginary part of the shell's refractive index across the considered range (Fig. S5), consistent with expectations that scattering is primarily governed by particle size and refractive index contrast rather than absorption.

3.2 Comparison of coated BC sphere with OC sphere

In order to gain further insights into the optical properties of coated BC, its optical properties were compared with OC spheres having the same physical dimension. For this comparison, the ratio R_{abs} of absorption cross-section of the coated BC and that of standalone OC with the same diameter was considered. Similarly, the ratio R_{sca} of scattering cross-section of the coated BC and that of standalone OC with the same diameter was estimated. Coating thickness can be expressed in terms of coating factor (CF), which is defined in this study as the ratio of the diameter of the coated sphere to the uncoated sphere. Figure 5, shows the changes in R_{abs} with CF for different core BC diameters. It can be seen that as the coating thickness is increased, the R_{abs} approaches 1, irrespective of the core diameter. Figure 6, shows the changes in R_{sca} with CF for different core BC diameters. Similar to R_{abs}, R_{sca} also approaches 1 with the increase in CF. However, the rate of approach to 1 is faster for R_{sca} compared to R_{abs}. Thus for a given BC

core diameter, as the OC coating increases, the optical properties inclusive of absorption and scattering part for the overall particle converges to those of the OC particle having the same dimension. It implies that the core BC gradually loses its optical significance as the OC coating increases. As seen from Fig. 5, when the CF increases above 15, the absorption properties of coated BC and pure OC are almost alike. Similarly, the difference in scattering properties of coated BC and standalone OC becomes insignificant when CF increases above 4. Although such high coating factors have not been reported in real-world scenarios, they may be theoretically plausible for ultrafine BC cores with diameters of just a few nanometers. These results indicate that as the OC coating on BC becomes thicker, the optical signature of the BC core contributes progressively less to the overall particle optical properties. Consequently, under conditions of substantial coating thickness, the particle may be optically approximated as a pure OC particle, neglecting the BC core depending on the coating factor. However, these modeling results should be interpreted cautiously and warrant further validation through laboratory measurements and simulations using more realistic, fractal-like BC morphologies rather than the idealized core–shell approximation.

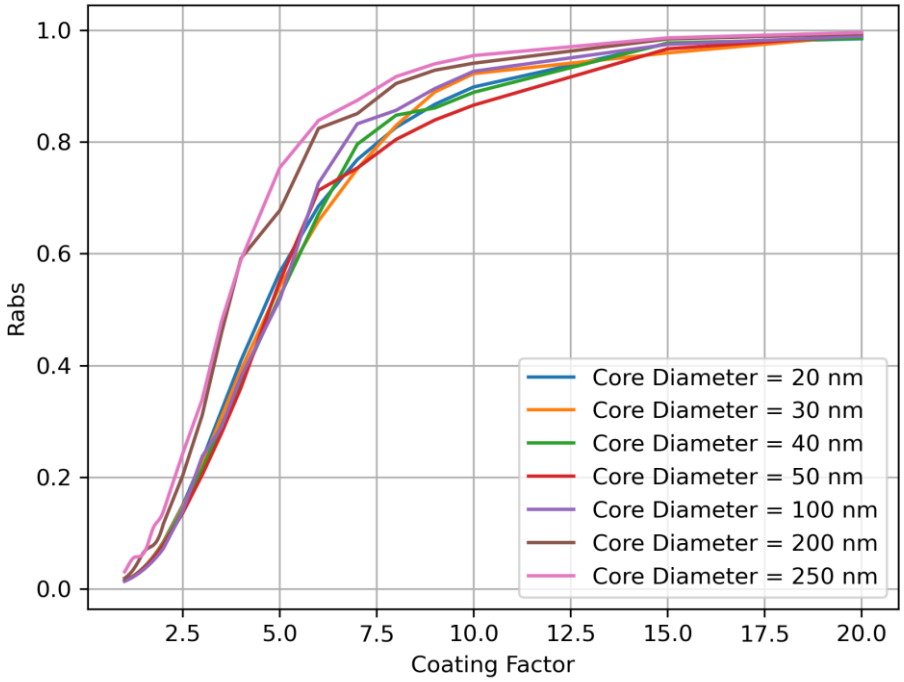

Fig. 5 Effect of coating factor on ratio R_{abs} of absortion crosssection of solid organic carbon and coated black carbon sphere at different core diameteres

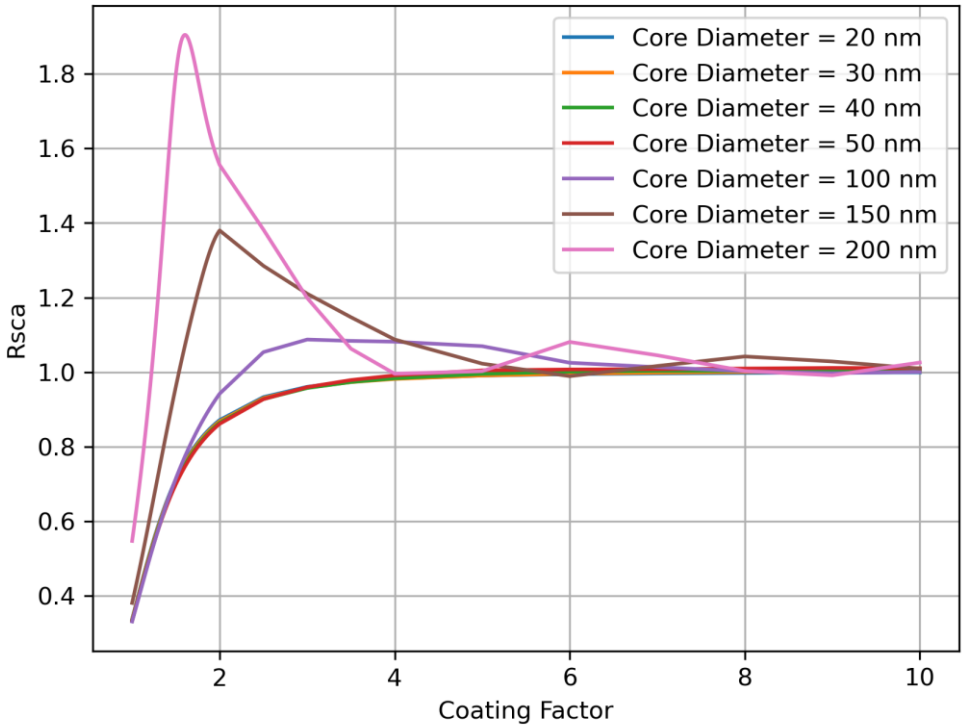

Fig. 6 Effect of coating factor on ratio R_{sca} of scattering crosssection of solid organic carbon and coated black carbon sphere at different core diameteres

3.3 Implications on radiative forcing potential

The SFE at 550 nm was estimated for coated BC spheres for various configuration of core and coat thicknesses using Eq. 4. The β was calculated directly from Mie theory using PyMieScatt, defined as the ratio of backscattering to total scattering cross-section ($\beta = C_{back} / C_{sca}$). Physically, β represents the fraction of incident light scattered into the backward direction, as described by Bohren and Huffman, 2008 [33]. The value of β depends on particle size, coating thickness, and refractive index contrast, and thus varies for each configuration considered. In our simulations at 550 nm, β values are presented in Fig. 7a. As expected, β decreases with increasing coating factor for a given BC core size, reflecting the enhanced forward scattering for larger or more heavily coated particles. MAC and MSC required for the calculation of SFE were also estimated using Mie calculations by normalizing the optical cross-section by their respective masses. Fig. 7b and 7c, illustrate the variations in MAC and MSC, respectively, as a function of the coating factor. MAC value for uncoated BC sphere CF = 1 was found to be vary from 4.8 to 7.1 m^2 g^{-1} depending on the BC diameter. This range aligns with the MAC values reported for BC calculated using Mie theory [34, 37, 40]. MAC for uncoated BC obtained in this study was found to be increasing with the diameter. The trend is consistent with existing literature, as MAC is expected to increase with diameter up to certain diameter before decreasing in magnitude [40, 41]. With respect to coating factor, MAC for the coated BC sphere was found to decrease with increase in organic coating thickness as shown in Fig. 7b. Conversely, it was found that MSC for the coated BC sphere increased with thicker coatings as seen in Fig. 7c. This behaviour can be attributed to the altered optical properties resulting from the introduction of organic coatings, which modifies the overall composition of the particle.

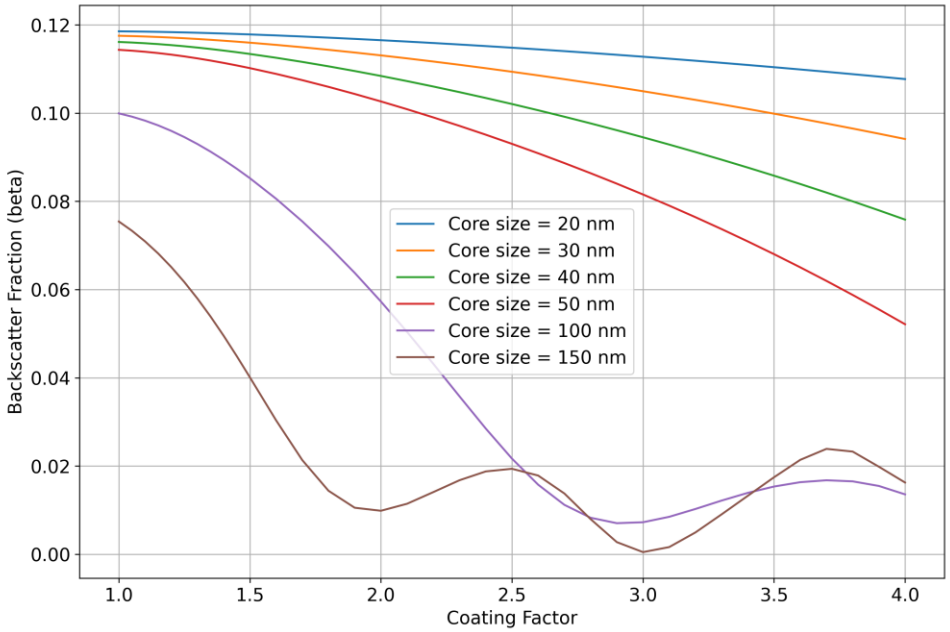
Backscatter Fraction (beta)
Coating Factor
Core size = 20 nm
Core size = 30 nm
Core size = 40 nm
Core size = 50 nm
Core size = 100 nm
Core size = 150 nm

(a)

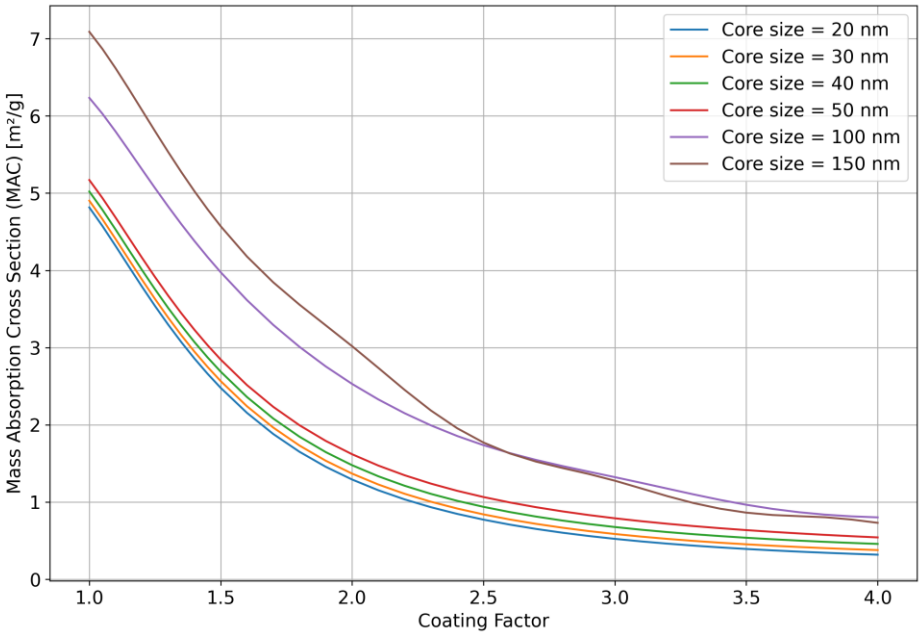
Mass Absorption Cross Section (MAC) [m²/g]
Coating Factor
Core size = 20 nm
Core size = 30 nm
Core size = 40 nm
Core size = 50 nm
Core size = 100 nm
Core size = 150 nm

(b)

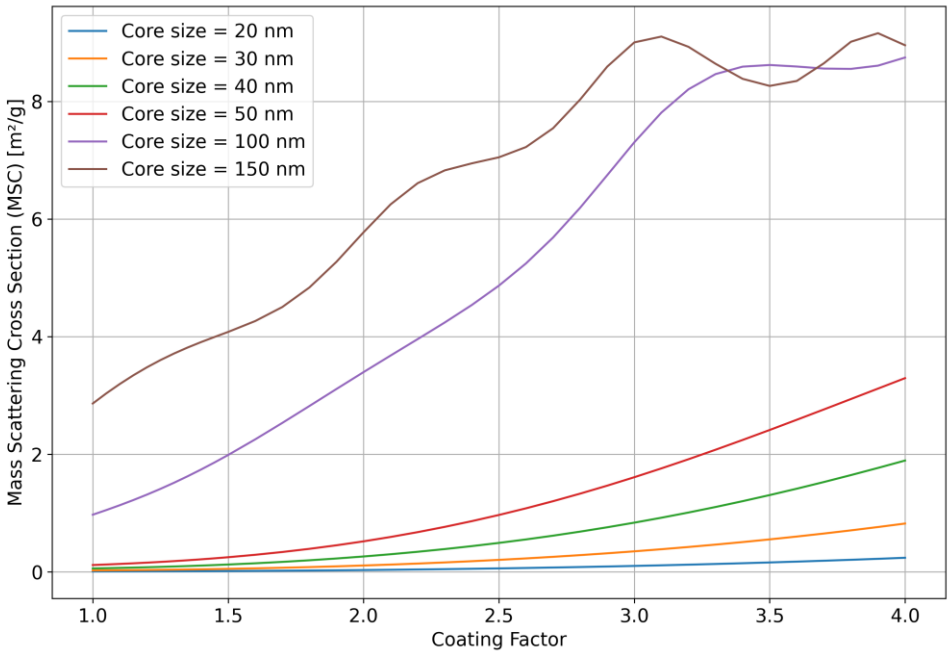

(c)

Fig. 7 Variation in (a) backscatter fraction (β), (b) mass absorption cross-section and (c) mass scattering cross-section with changes in coating factor for given black carbon core diameters

The variation of SFE with coating factor for different BC core diameters at 550 nm is shown in Fig. 8, and at 350, 450, and 650 nm in Fig. S6 (Supplementary Information). As the thickness of the OC coating on BC increases, the SFE of the coated particles decreases irrespective of the core diameter. This reduction in SFE results from the combined influence of absorption and scattering enhancements induced by the organic coating. Although both absorption and scattering cross-sections increase with coating, the enhancement in scattering is more pronounced, leading to an overall rise in single scattering albedo (SSA) and, consequently, a reduction in SFE, as discussed in Section 3.1. Since radiative forcing is highly sensitive to variations in SSA, this increase in scattering diminishes the net forcing effect of coated BC [42]. For instance, for a 100 nm BC core, an increase in coating factor from 1 to 3 reduces the SFE by nearly 80%. This implies that in real-world scenarios, where BC particles are frequently encapsulated by organic coatings, their radiative forcing impact may be less significant than previously estimated. Hence, considering only absorption enhancement while neglecting the concurrent increase in scattering due to organic coatings can lead to an overestimation of the radiative forcing potential of coated BC. These findings hold important implications for climate models and the accurate representation of aerosol–radiation interactions in the Earth's energy budget.

The magnitude of SFE at any coating factor was found to decrease with increasing wavelength, consistent with the stronger absorption of OC at shorter wavelengths. To isolate the effect of wavelength-dependent shell absorption, SFE values for absorbing and non-absorbing shells (κ_{OC} = 0.00001) were computed for a 120 nm BC core at four wavelengths (350, 450, 550, and 650 nm) and are shown in Fig. 9. Across all coating factors, the absorbing-shell cases exhibited

359 consistently higher SFE values than their non-absorbing counterparts. The difference between
360 the two increased with coating factor and was more pronounced at shorter wavelengths,
361 reflecting the stronger absorption of OC in the near-UV region. At longer wavelengths, where
362 OC absorption weakens, the difference in SFE between absorbing and non-absorbing shells
363 became smaller.

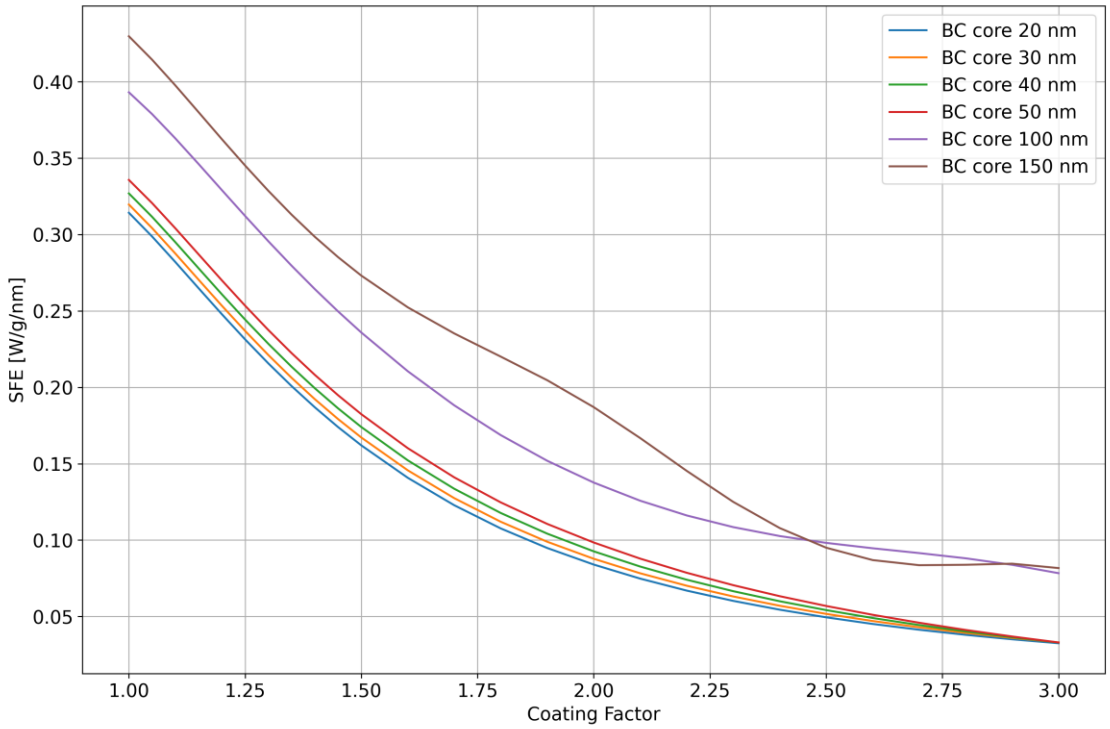

364

365 Fig. 8 Variation in simple forcing efficiency with changes in coating factor for given black
366 carbon core diameters at 550 nm wavelength

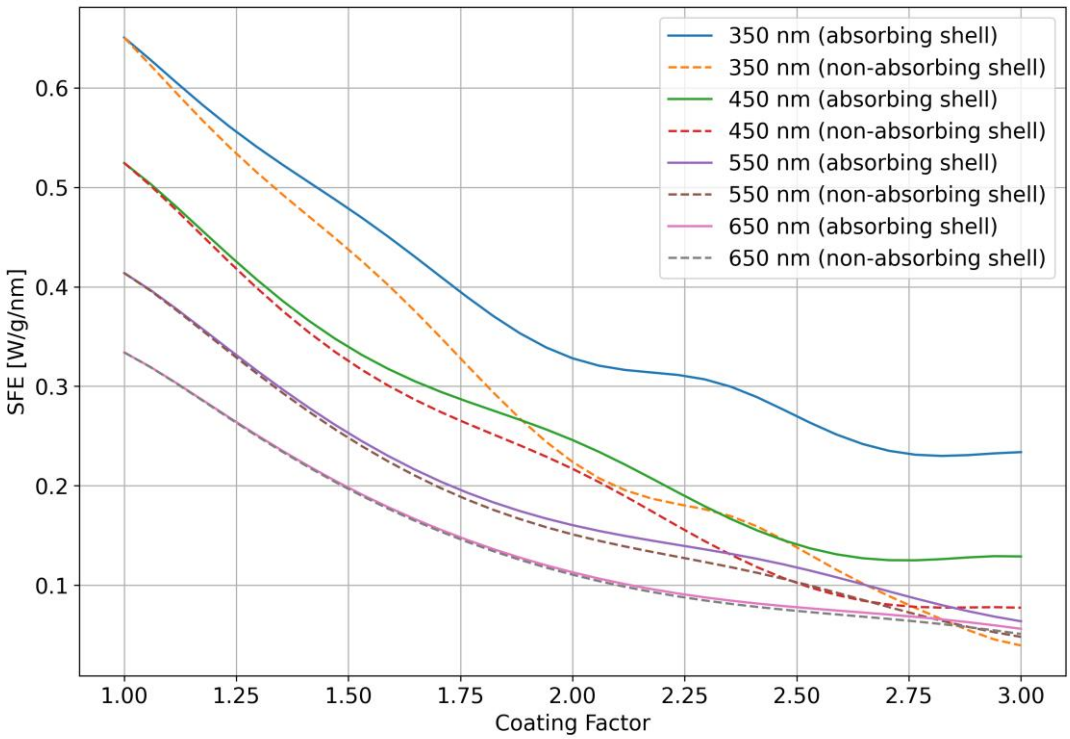

Figure 9 Variation of simple forcing efficiency (SFE) with coating factor for a 120 nm BC core at four wavelengths (350, 450, 550, and 650 nm). Solid lines represent the case of an absorbing organic shell (imaginary refractive index, κ_{OC} = 0.0726, 0.0210, 0.0083, and 0.0028 at 350, 450, 550, and 650 nm, respectively), while dashed lines denote a non-absorbing shell (κ_{OC} = 0.00001).

4. Conclusion

The study demonstrates the significant influence of coating thickness and core size on the optical properties of BC sphere. The results reveal that both the absorption and scattering cross-sections of coated BC particles are enhanced compared to uncoated BC, primarily due to the lensing effect and the increased physical dimension due the coating. The enhancement in scattering was more pronounced compared to absorption, highlighting the critical role of coating thickness in modulating the scattering properties of BC aerosols. The study finds that very thick organic coatings can reduce the optical significance of BC core lowering its relative contribution to overall absorption and scattering. The SFE of coated BC was found to decrease with increasing coating thickness, suggesting less pronounced impact on radiative forcing in real-world scenarios where BC particles are usually coated with organic material. Overall, these insights emphasize the need for careful consideration of coating effects on the optical properties of BC for assessment of its impact on radiative forcing.

Author statement

T.D. Rathod: Writing – original draft, Conceptualization, Formal analysis, Methodology.

S.K. Sahu: Writing - review & editing, Formal analysis, Supervision.

Declarations

Funding: The authors declare that no funding was received for the conduct of this research.

Conflict of Interest: The authors declare no competing interests.

References

1. Szopa, S., Naik, V., Adhikary, B., Artaxo, P., Berntsen, T., Collins, W. D., ... & Zanis, P. (2023). Short-Lived Climate Forcers (Chapter 6). IPCC 2021: Climate Change 2021: The Physical Science Basis. Contribution of Working Group I to the Sixth Assessment Report of the Intergovernmental Panel on Climate Change, *817-922*.
2. Bond, T. C., Doherty, S. J., Fahey, D. W., Forster, P. M., Berntsen, T., DeAngelo, B. J., Flanner, M. G., Ghan, S., Kärcher, B., Koch, D., & Kinne, S. (2013). Bounding the role of black carbon in the climate system: A scientific assessment. *Journal of Geophysical Research: Atmospheres, 118*, 5380–5552. https://doi.org/10.1002/jgrd.50171
3. Liu, D., Whitehead, J., Alfarra, M. R., Reyes-Villegas, E., Spracklen, D. V., Reddington, C. L., Kong, S., Williams, P. I., Ting, Y. C., Haslett, S., & Taylor, J. W. (2017). Black-carbon absorption enhancement in the atmosphere determined by particle mixing state. *Nature Geoscience, 10*, 184–188. https://doi.org/10.1038/ngeo2901
4. Zhang, Y., Favez, O., Canonaco, F., Liu, D., Močnik, G., Amodeo, T., Sciare, J., Prévôt, A. S., Gros, V., & Albinet, A. (2018). Evidence of major secondary organic aerosol contribution to lensing effect black carbon absorption enhancement. *npj Climate and Atmospheric Science, 1*, 47. https://doi.org/10.1038/s41612-018-0056-2
5. Huang, X.-F., Peng, Y., Wei, J., Peng, J., Lin, X.-Y., Tang, M.-X., Cheng, Y., Men, Z., Fang, T., Zhang, J., He, L.-Y., Cao, L.-M., Liu, C., Zhang, C., Mao, H., Seinfeld, J. H., & Wang, Y. (2024). Microphysical complexity of black carbon particles restricts their warming potential. *One Earth, 7*, 136–145. https://doi.org/10.1016/j.oneear.2023.12.004
6. Stocker, T. F., Qin, D., Plattner, G. K., Tignor, M. M., Allen, S. K., Boschung, J., ... Midgley, P. M. (2014). *Climate change 2013: The physical science basis. Contribution of Working Group I to the Fifth Assessment Report of the Intergovernmental Panel on Climate Change*. Intergovernmental Panel on Climate Change (IPCC).
7. Hu, K., Liu, D., Tian, P., Wu, Y., Li, S., Zhao, D., Li, R., Sheng, J., Huang, M., Ding, D., & Liu, Q. (2022). Identifying the fraction of core–shell black carbon particles in a complex mixture to constrain the absorption enhancement by coatings. *Environmental Science & Technology Letters, 9*, 272–279. https://doi.org/10.1021/acs.estlett.2c00060
8. Zhai, J., Yang, X., Li, L., Bai, B., Liu, P., Huang, Y., Fu, T. M., Zhu, L., Zeng, Z., Tao, S., & Lu, X. (2022). Absorption enhancement of black carbon aerosols constrained by mixing-state heterogeneity. *Environmental Science & Technology, 56*, 1586–1593. https://doi.org/10.1021/acs.est.1c06180
9. Jacobson, M. Z. (2001). Strong radiative heating due to the mixing state of black carbon in atmospheric aerosols. *Nature, 409*, 695–697. https://doi.org/10.1038/35055518
10. Bond, T. C., Habib, G., & Bergstrom, R. W. (2006). Limitations in the enhancement of visible light absorption due to mixing state. *Journal of Geophysical Research: Atmospheres, 111*, D20211. https://doi.org/10.1029/2006JD007315
11. Lack, D. A., & Cappa, C. D. (2010). Impact of brown and clear carbon on light absorption enhancement, single scatter albedo, and absorption wavelength dependence of black carbon. *Atmospheric Chemistry and Physics, 10*, 4207–4220. https://doi.org/10.5194/acp-10-4207-2010
12. Rathod, T. D., Sahu, S. K., Tiwari, M., Bhangare, R. C., & Ajmal, P. Y. (2021). Light absorption enhancement due to mixing in black carbon and organic carbon generated

during biomass burning. *Atmospheric Pollution Research, 12*, 101236. https://doi.org/10.1016/j.apr.2021.101236

13. Shiraiwa, M., Kondo, Y., Moteki, N., Takegawa, N., Miyazaki, Y., & Kita, K. (2008). Radiative impact of mixing state of black carbon aerosol in Asian outflow. *Journal of Geophysical Research: Atmospheres, 113*, D24210. https://doi.org/10.1029/2008JD010546
14. Wang, Y., Li, W., Huang, J., Liu, L., Pang, Y., He, C., Liu, F., Liu, D., Bi, L., Zhang, X., & Shi, Z. (2021). Nonlinear enhancement of radiative absorption by black carbon in response to particle mixing structure. *Geophysical Research Letters, 48*(24), e2021GL096437. https://doi.org/10.1029/2021GL096437
15. Liu, S., Aiken, A. C., Gorkowski, K., Dubey, M. K., Cappa, C. D., Williams, L. R., Herndon, S. C., Massoli, P., Fortner, E. C., Chhabra, P. S., & Brooks, W. A. (2015). Enhanced light absorption by mixed source black and brown carbon particles in UK winter. *Nature Communications, 6*, 8435. https://doi.org/10.1038/ncomms9435
16. Lefevre, G., Yon, J., Bouvier, M., Liu, F., & Coppalle, A. (2019). Impact of organic coating on soot angular and spectral scattering properties. *Environmental Science & Technology, 53*, 6383–6391. https://doi.org/10.1021/acs.est.8b05482
17. Lefevre, G., Yon, J., Liu, F., & Coppalle, A. (2018). Spectrally resolved light extinction enhancement of coated soot particles. *Atmospheric Environment, 186*, 89–101. https://doi.org/10.1016/j.atmosenv.2018.05.029
18. Yuan, C., Zheng, J., Ma, Y., Jiang, Y., Li, Y., & Wang, Z. (2020). Significant restructuring and light absorption enhancement of black carbon particles by ammonium nitrate coating. *Environmental Pollution, 262*, 114172. https://doi.org/10.1016/j.envpol.2020.114172
19. Wang, X., Heald, C. L., Ridley, D. A., Schwarz, J. P., Spackman, J. R., Perring, A. E., Coe, H., Liu, D., & Clarke, A. D. (2014). Exploiting simultaneous observational constraints on mass and absorption to estimate the global direct radiative forcing of black carbon and brown carbon. *Atmospheric Chemistry and Physics, 14*, 10989–11010. https://doi.org/10.5194/acp-14-10989-2014
20. Sumlin, B. J., Heinson, W. R., & Chakrabarty, R. K. (2018). Retrieving the aerosol complex refractive index using PyMieScatt: A Mie computational package with visualization capabilities. *Journal of Quantitative Spectroscopy and Radiative Transfer, 205*, 127–134. https://doi.org/10.1016/j.jqsrt.2017.10.012
21. Wang, Y., Liu, F., He, C., Bi, L., Cheng, T., Wang, Z., ... & Li, W. (2017). Fractal dimensions and mixing structures of soot particles during atmospheric processing. *Environmental Science & Technology Letters*, *4(11)*, 487-493.
22. Kahnert, M., & Kanngießer, F. (2020). Modelling optical properties of atmospheric black carbon aerosols. *Journal of Quantitative Spectroscopy and Radiative Transfer, 244*, 106849. https://doi.org/10.1016/j.jqsrt.2020.106849
23. Matsui, H., Hamilton, D. S., & Mahowald, N. M. (2018). Black carbon radiative effects highly sensitive to emitted particle size when resolving mixing-state diversity. *Nature communications*, *9(1)*, 3446.
24. Wu, Y., Cheng, T., Liu, D., Allan, J. D., Zheng, L., & Chen, H. (2018). Light absorption enhancement of black carbon aerosol constrained by particle morphology. *Environmental science & technology*, *52(12)*, 6912-6919.
25. Cappa, C. D., Zhang, X., Russell, L. M., Collier, S., Lee, A. K., Chen, C. L., ... & Zhang, Q. (2019). Light absorption by ambient black and brown carbon and its dependence on

484 black carbon coating state for two California, USA, cities in winter and summer.
485 *Journal of Geophysical Research: Atmospheres*, *124(3)*, 1550-1577.
486 26. Liu, J., Wang, G., Zhu, C., Zhou, D., & Wang, L. (2023). Numerical investigation on
487 retrieval errors of mixing states of fractal black carbon aerosols using single-particle
488 soot photometer based on Mie scattering and the effects on radiative forcing estimation.
489 *Atmospheric Measurement Techniques*, *16(20)*, 4961-4974.
490 27. Sumlin, B. J., Pandey, A., Walker, M. J., Pattison, R. S., Williams, B. J., & Chakrabarty,
491 R. K. (2017). Atmospheric photooxidation diminishes light absorption by primary
492 brown carbon aerosol from biomass burning. *Environmental Science & Technology*
493 *Letters*, *4(12)*, 540-545.
494 28. Womack, C. C., Manfred, K. M., Wagner, N. L., Adler, G., Franchin, A., Lamb, K. D.,
495 ... & Washenfelder, R. A. (2020). Complex refractive indices in the ultraviolet and
496 visible spectral region for highly absorbing non-spherical biomass burning aerosol.
497 *Atmospheric Chemistry and Physics Discussions*, *2020*, 1-29.
498 29. Hoffer, A., Gelencsér, A., Blazso, M., Guyon, P., Artaxo, P., & Andreae, M. O. (2006).
499 Diel and seasonal variations in the chemical composition of biomass burning aerosol.
500 *Atmospheric Chemistry and Physics*, *6(11)*, 3505-3515.
501 30. Feng, Y., Ramanathan, V., & Kotamarthi, V. R. (2013). Brown carbon: A significant
502 atmospheric absorber of solar radiation? *Atmospheric Chemistry and Physics, 13*,
503 8607–8621. https://doi.org/10.5194/acp-13-8607-2013
504 31. Cappa, C. D., Onasch, T. B., Massoli, P., Worsnop, D. R., Bates, T. S., Cross, E. S., &
505 Davidovits, P. (2012). Radiative absorption enhancements due to the mixing state of
506 atmospheric black carbon. *Science, 337*, 1078–1081.
507 https://doi.org/10.1126/science.1223447
508 32. Luo, J., Zhang, Y., Wang, F., & Zhang, Q. (2018). Effects of brown coatings on the
509 absorption enhancement of black carbon: A numerical investigation. *Atmospheric*
510 *Chemistry and Physics, 18*, 16897–16914. https://doi.org/10.5194/acp-18-16897-2018
511 33. Bohren, C. F., & Huffman, D. R. (2008). *Absorption and scattering of light by small*
512 *particles*. John Wiley & Sons.
513 34. Bond, T. C., & Bergstrom, R. W. (2006). Light absorption by carbonaceous particles:
514 An investigative review. *Aerosol Science and Technology, 40*, 27–67.
515 https://doi.org/10.1080/02786820500421521
516 35. Chen, Y.: Characterization of carbonaceous aerosols from biofuel combustion:
517 emissions and climate relevant properties, Doctoral Dissertation, University of Illinois
518 Urbana Champaign, Illinois Digital Environment for Access to Learning and
519 Scholarship, 215 pp., 2011
520 36. Schkolnik, G., Chand, D., Hoffer, A., Andreae, M. O., Erlick, C., Swietlicki, E., &
521 Rudich, Y. (2015). Constraining the density and complex refractive index of elemental
522 carbon and organic carbon particles: A comparison of techniques and implications for
523 absorption enhancement. *Atmospheric Chemistry and Physics, 15*, 2959–2974.
524 https://doi.org/10.1016/j.atmosenv.2006.09.035
525 37. Zhang, Y., Zhang, Q., Cheng, Y., Su, H., Li, H., Li, M., Zhang, X., Ding, A., & He, K.
526 (2018). Amplification of light absorption of black carbon associated with air pollution.
527 *Atmospheric Chemistry and Physics, 18*, 9879–9896. https://doi.org/10.5194/acp-18-
528 9879-2018
529 38. Wu, H., Taylor, J. W., Langridge, J. M., Yu, C., Allan, J. D., Szpek, K., ... & Coe, H.
530 (2021). Rapid transformation of ambient absorbing aerosols from West African biomass
531 burning. *Atmospheric Chemistry and Physics Discussions*, *2021*, 1-37.

39. Taylor, J. W., Wu, H., Szpek, K., Bower, K., Crawford, I., Flynn, M. J., ... & Coe, H. (2020). Absorption closure in highly aged biomass burning smoke. *Atmospheric Chemistry and Physics*, *20(19)*, 11201-11221.
40. Zhao, G., Tao, J., Kuang, Y., Shen, C., Yu, Y., & Zhao, C. (2019). Role of black carbon mass size distribution in the direct aerosol radiative forcing. *Atmospheric Chemistry and Physics, 19*, 13175–13188. https://doi.org/10.5194/acp-19-13175-2019
41. Cohen, D. D., Taha, G., Stelcer, E., Garton, D., & Box, G. (2000, November). The measurement and sources of fine particle elemental carbon at several key sites in NSW over the past eight years. In *Proceedings of 15th International Clean Air and Environment Conference* (pp. 485–490). Clean Air Society of Australia and New Zealand.
42. Takemura, T., Nakajima, T., Dubovik, O., Holben, B. N., & Kinne, S. (2002). Single-scattering albedo and radiative forcing of various aerosol species with a global three-dimensional model. *Journal of Climate, 15*, 333–352. https://doi.org/10.1175/1520-0442(2002)015<0333:SSAARF>2.0.CO;2

SUPPORTING INFORMATION

Effect of organic coatings on optical properties of black carbon aerosol: Insights from mie theory based model simulations

T.D. Rathod[1, 2] and S.K. Sahu[1, 2*]

[1]Environmental Monitoring and Assessment Division, Bhabha Atomic Research Centre, Trombay, Mumbai 400085

[2]Homi Bhabha National Institute, Anushakti Nagar Mumbai– 400094, India.

*Corresponding author: Tel: +912225592375

E-mail address: sksahu@barc.gov.in

Table S1 Imaginary part (κ) of the refractive index of organic carbon reported by previous studies at different wavelengths.

Wavelength (nm)	Kirchstetter et al. (2004)	Chen (2011) Low-T[1]	Chen (2011) Mid-T[1]	Chen (2011) High-T[1]	Feng et al. (2013)	Rathod et al. (2017, Wood)	Rathod et al. (2017, Dung cake)	Average κ
350	0.168	0.0499	0.0571	0.0971	0.075	0.0140	0.0470	**0.0726**
450	0.063	0.00635	0.0098	0.0274	0.020	0.0030	0.0250	**0.0210**
550	0.030	0.0015	0.0021	0.00545	0.003	0.0020	0.0150	**0.0083**
650	0.005	0.00147	0.0010	0.0027	0.0003	0.0010	0.0090	**0.0028**

[1] Low-T, Mid-T, and High-T refer to the organic carbon generated at different combustion temperatures in Chen (2011).

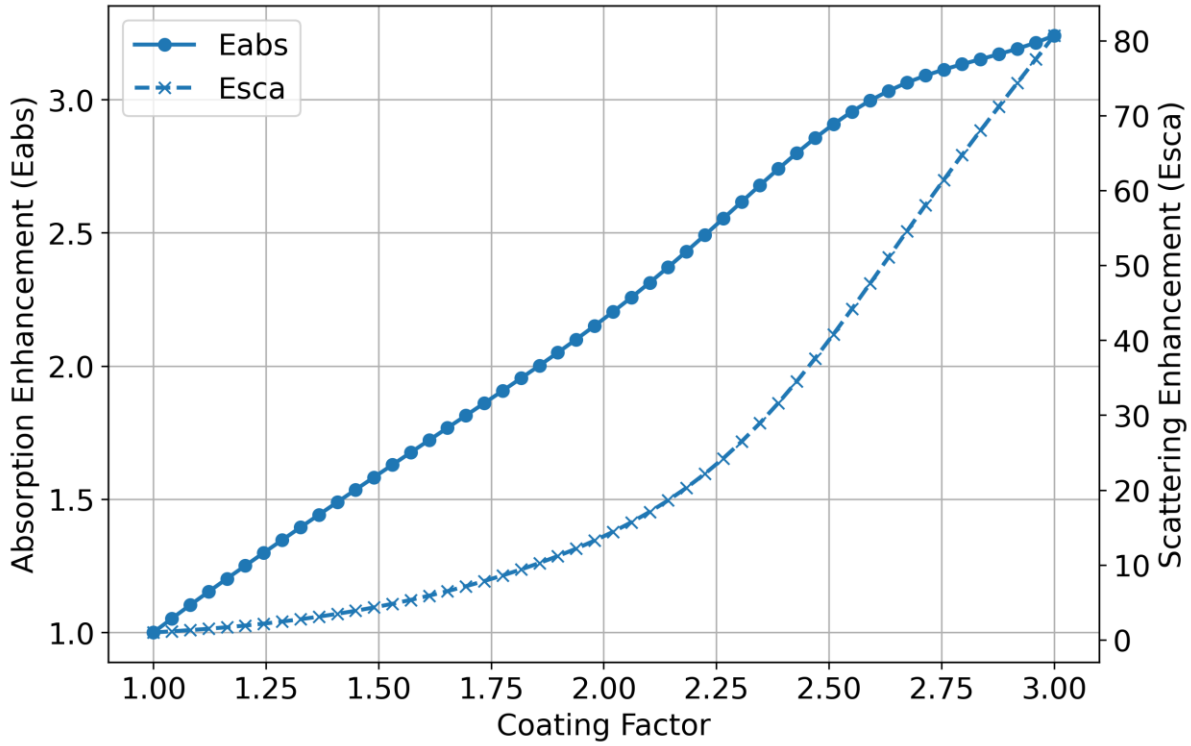

Fig. S1 Absorption (Eabs, left y-axis) and scattering (Esca, right y-axis) enhancement factors of core–shell particles with a 120 nm BC core as a function of coating factor at 550 nm.

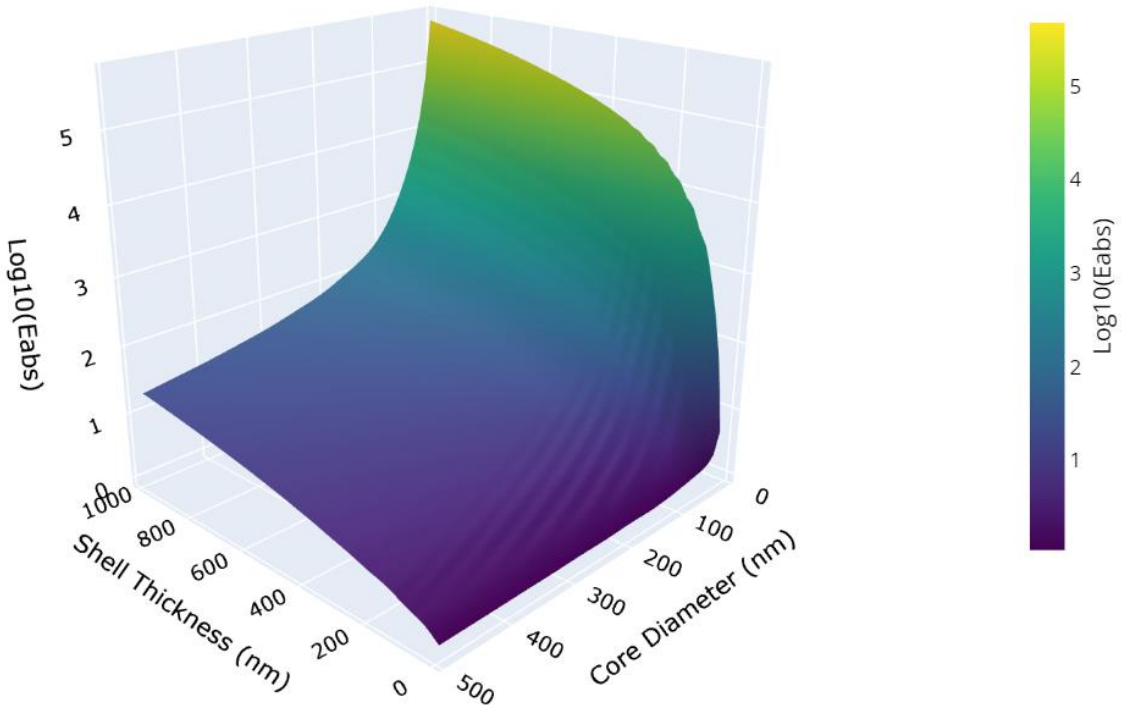

(a) 350 nm

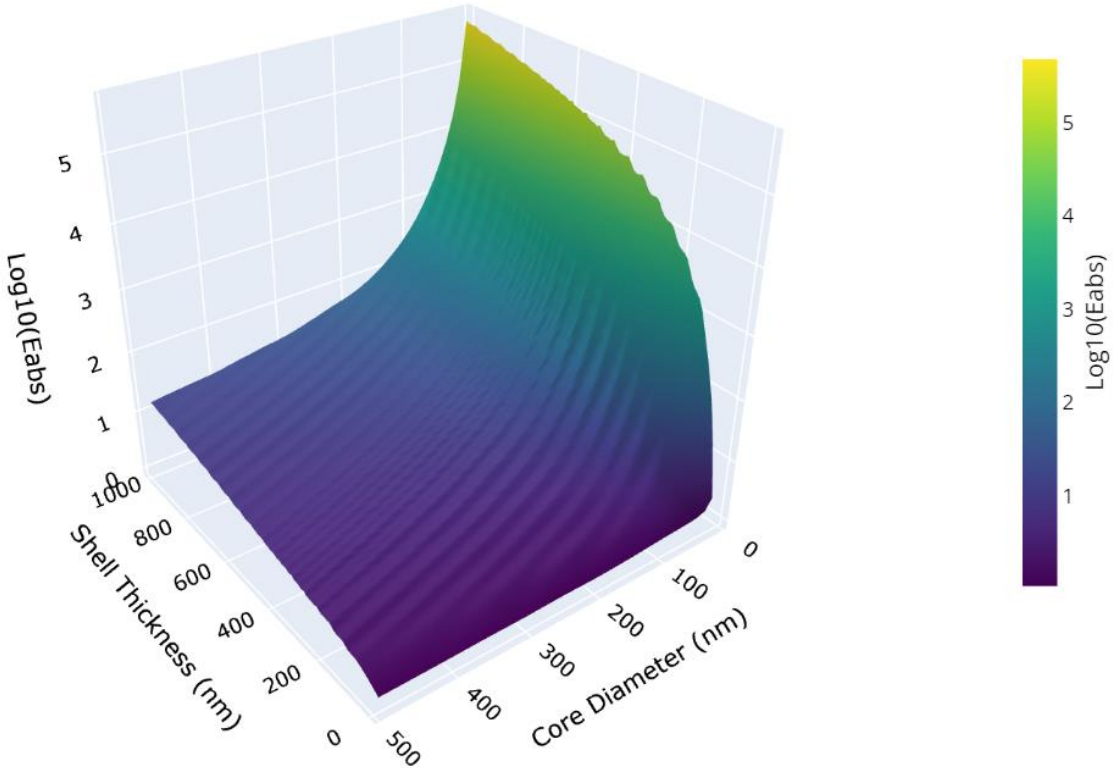

(b) 450 nm

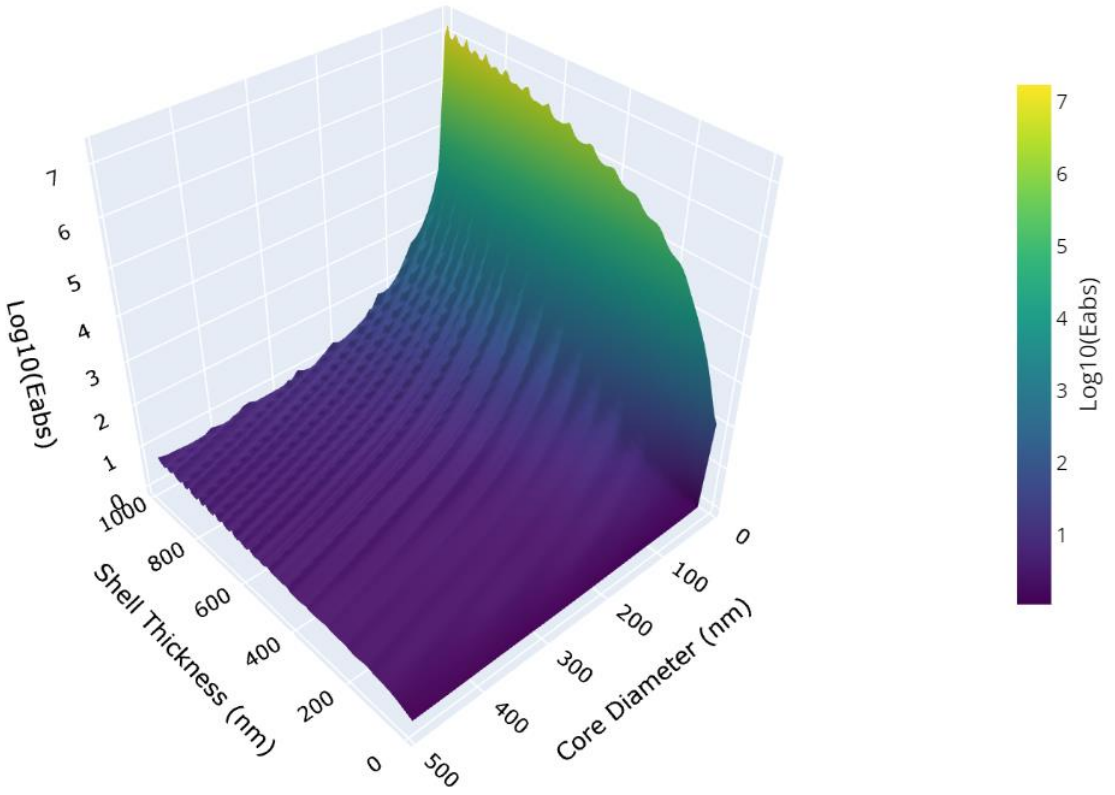

(c) 650 nm

Fig. S2 Enhancement in absorption cross-section due to organic coating on black carbon core at different wavelengths

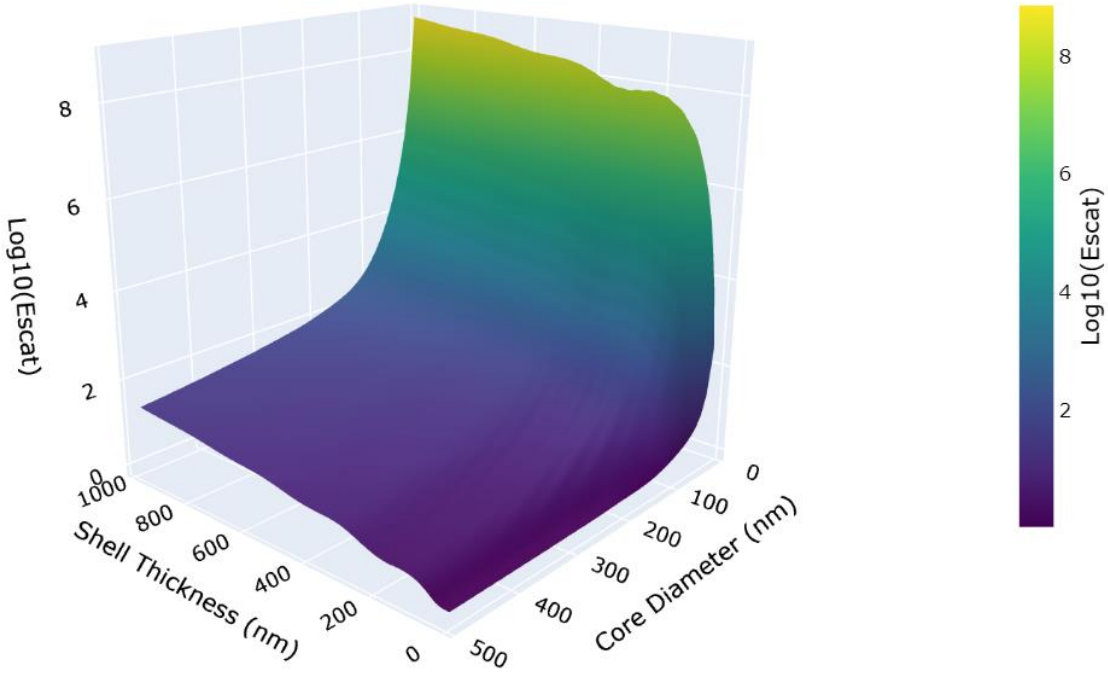

(a) 350 nm

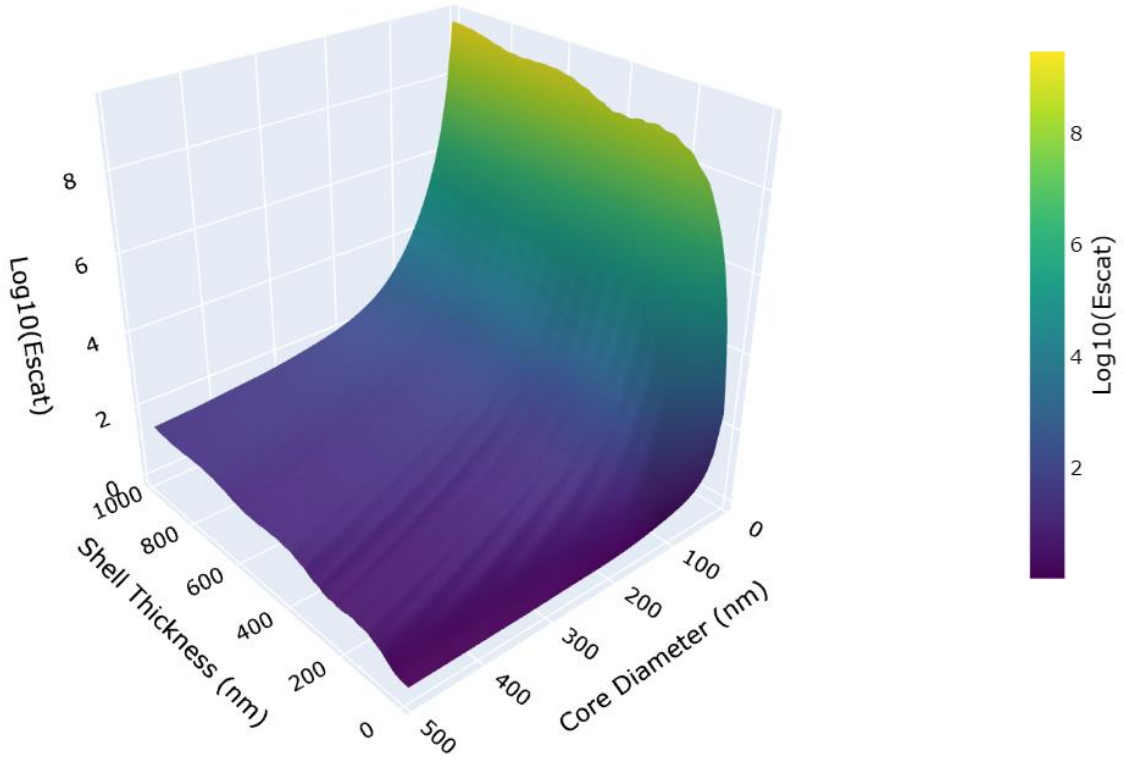

(b) 450 nm

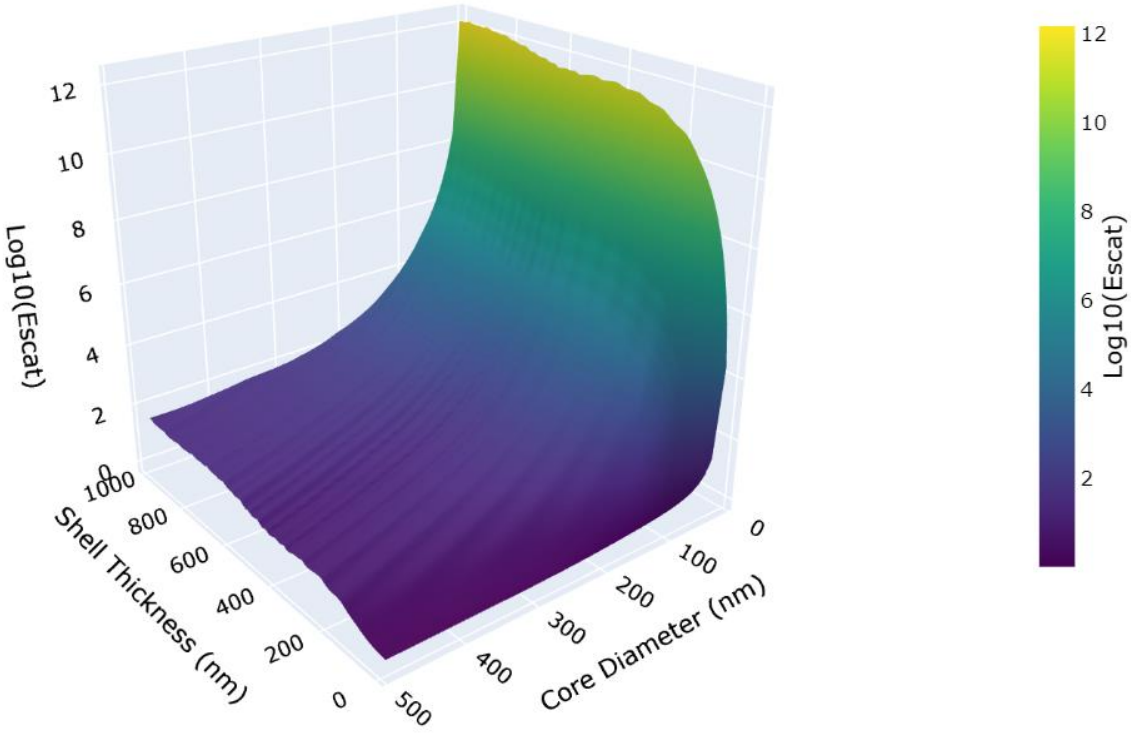

(c) 650 nm

Fig. S3 Enhancement in scattering cross-section due to organic coating on black carbon core at different wavelengths

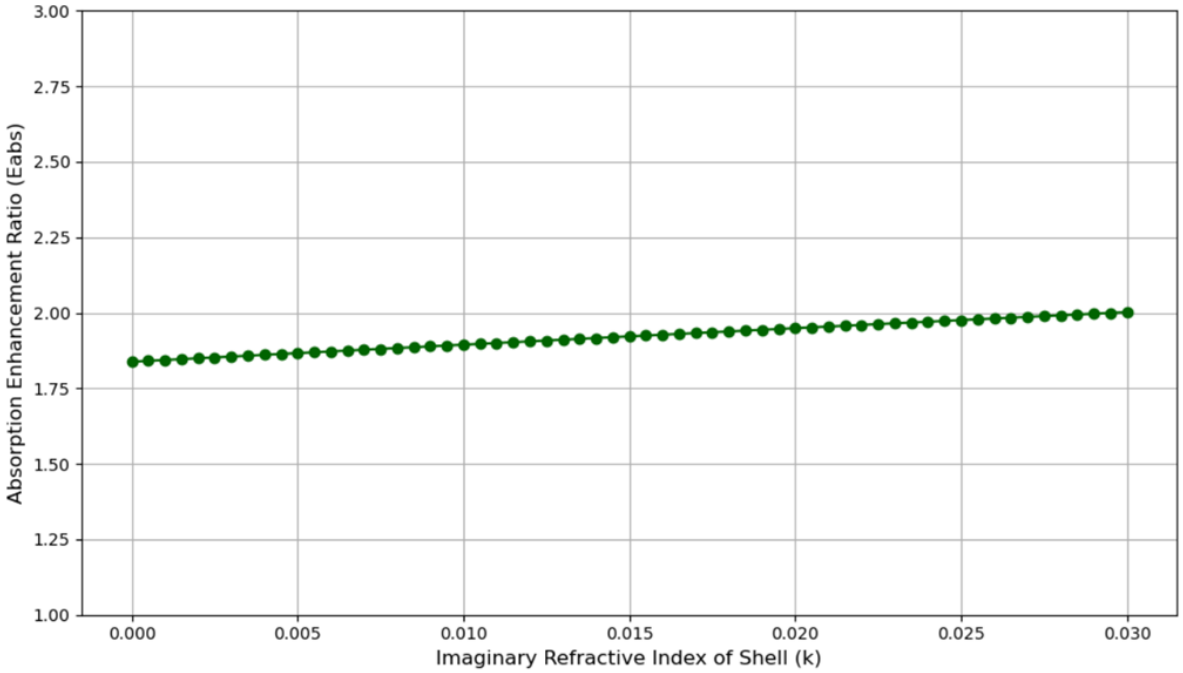

Fig. S4 Variation of Absorption Enhancement with Imaginary Refractive Index of Organic Coating for a Core–Shell Particle (Core Diameter = 150 nm, Shell Thickness = 50 nm)

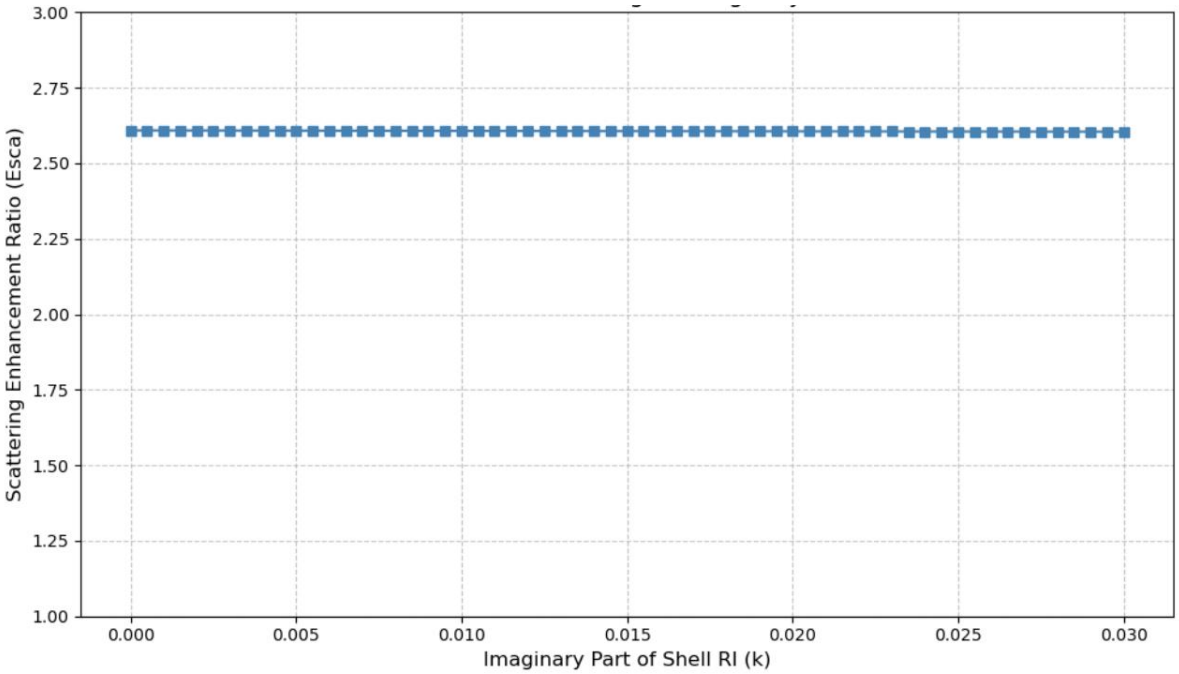

Fig. S5 Variation of Scattering Enhancement with Imaginary Refractive Index of Organic Coating for a Core–Shell Particle (Core Diameter = 150 nm, Shell Thickness = 50 nm)

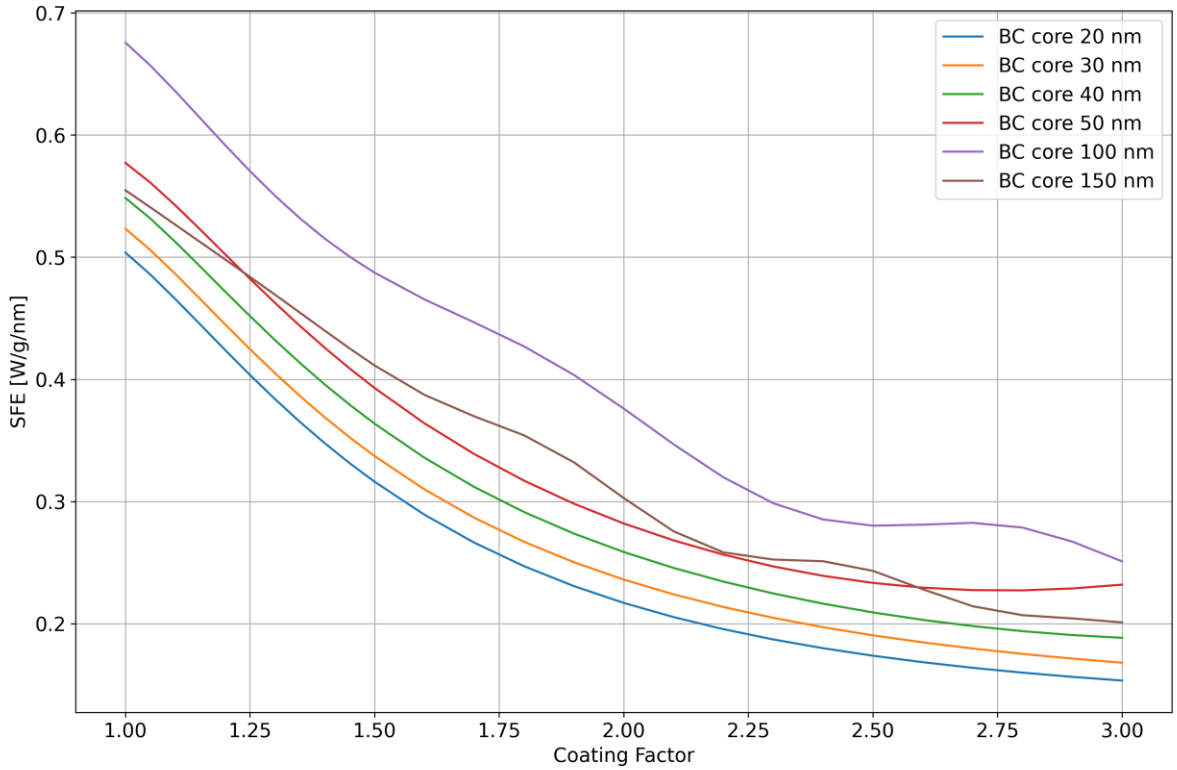
BC core 20 nm
BC core 30 nm
BC core 40 nm
BC core 50 nm
BC core 100 nm
BC core 150 nm
SFE [W/g/nm]
Coating Factor
0.7
0.6
0.5
0.4
0.3
0.2
1.00
1.25
1.50
1.75
2.00
2.25
2.50
2.75
3.00

(a)

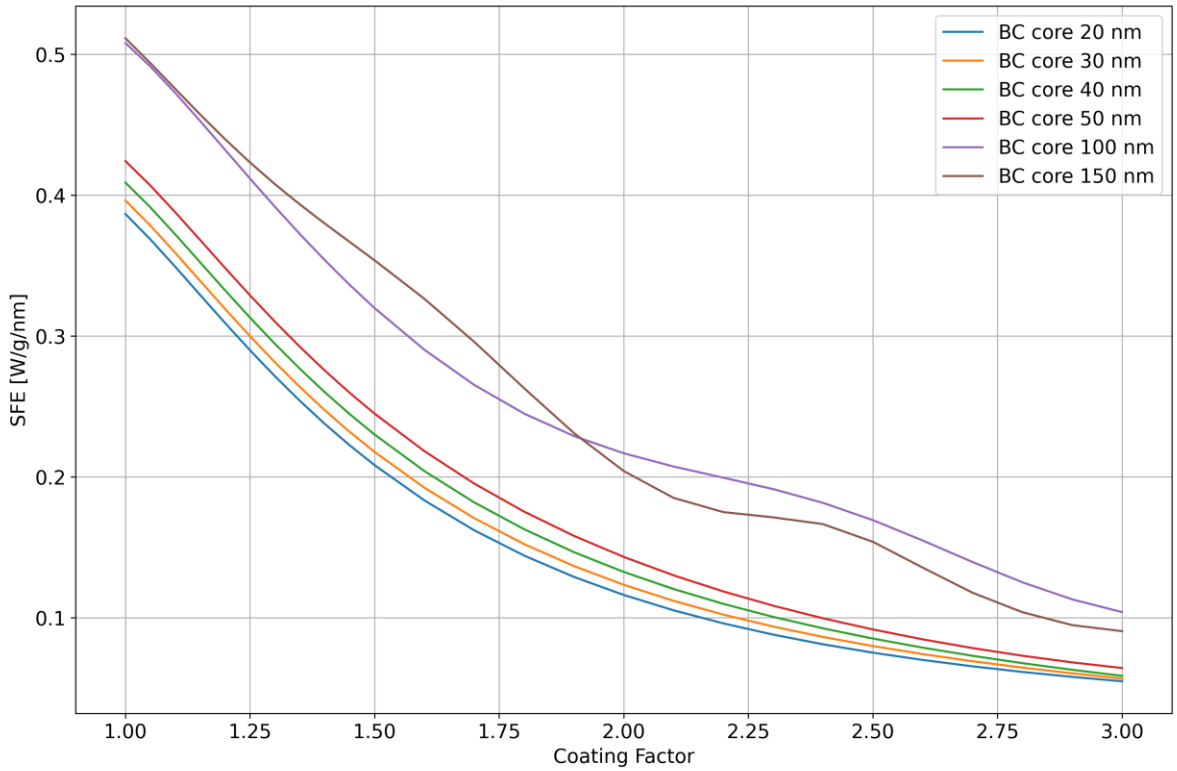
BC core 20 nm
BC core 30 nm
BC core 40 nm
BC core 50 nm
BC core 100 nm
BC core 150 nm
SFE [W/g/nm]
Coating Factor
0.5
0.4
0.3
0.2
0.1
1.00
1.25
1.50
1.75
2.00
2.25
2.50
2.75
3.00

(b)

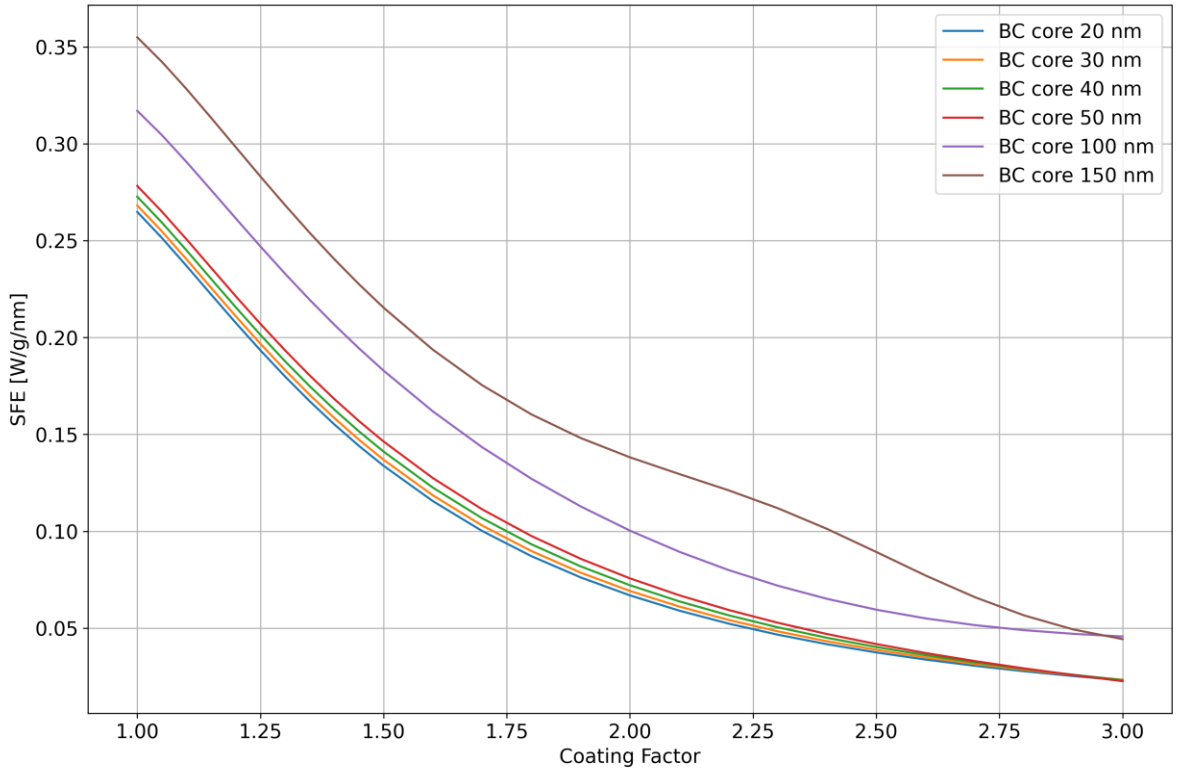

(c)

Fig. S6 Simple Forcing Efficiency (SFE) of black carbon (BC) cores coated with organic carbon (OC) as a function of coating factor for different BC core sizes at three wavelengths: (a) 350 nm, (b) 450 nm, and (c) 650 nm.

References

Rathod, T., Sahu, S. K., Tiwari, M., Yousaf, A., Bhangare, R. C., & Pandit, G. G. (2017). Light absorbing properties of brown carbon generated from pyrolytic combustion of household biofuels. *Aerosol and Air Quality Research*, *17*, 108–116. https://doi.org/10.4209/aaqr.2015.11.0639

Chen, Y.: Characterization of carbonaceous aerosols from biofuel combustion: emissions and climate relevant properties, Doctoral Dissertation, University of Illinois Urbana Champaign, Illinois Digital Environment for Access to Learning and Scholarship, 215 pp., 2011

Hoffer, A., Gelencsér, A., Blazso, M., Guyon, P., Artaxo, P., & Andreae, M. O. (2006). Diel and seasonal variations in the chemical composition of biomass burning aerosol. *Atmospheric Chemistry and Physics*, *6(11)*, 3505-3515.

Feng, Y., Ramanathan, V., & Kotamarthi, V. R. (2013). Brown carbon: A significant atmospheric absorber of solar radiation? *Atmospheric Chemistry and Physics*, *13*, 8607–8621. https://doi.org/10.5194/acp-13-8607-2013

Kirchstetter, T. W., Novakov, T., & Hobbs, P. V. (2004). Evidence that the spectral dependence of light absorption by aerosols is affected by organic carbon. *Journal of Geophysical Research: Atmospheres*, *109*(D21).